Multinomial Bubble Score Model

Peter Tikuisis[1] and Keith A. Gault[2]
[1]Defence and Civil Institute of Environmental Medicine, Toronto, Canada M3M 3B9
[2]Navy Experimental Diving Unit, Panama City, FL

Model Demonstration

I would like to acknowledge Keith Gault , my co-author, as the person who conducted most of this research for his Master's degree.

It is generally accepted that bubbles are the precursors to decompression sickness (DCS) although the exact linkage between the two is not known. Bubble models are increasingly being used to predict DCS. We propose that the best test of a bubble model is to apply it against data that measure bubbles directly. This presentation will focus on the development of a model to predict the occurrence of bubbles as measured using Doppler ultrasound techniques.

Data

The data were obtained from measurement sites on the precordium, the left subclavian, and right subclavian of the diver's body at rest and exercise during and after a dive. Measurements were taken approximately every 30 to 40 min. Signals were graded according to frequency, duration, and amplitude, and converted into a single bubble grade, BG, ranging from zero indicating no bubble activity to four indicating maximum bubble activity using the Kisman-Masurel code (Nishi 1993). The resultant data are multinomal and categorical.

Both air and helium-oxygen (heliox) dives conducted at DCIEM were used in this study (see Table 1). The more than 2,000 man-dives in the data set included a variety of dives, single and repetitive, and some with oxygen decompression.

Table 1. Summary of dive data with BG recordings.

	Air	Heliox
Number of Trials	276	86
Number of man-dives	1,425	639
Bottom Depth (msw)	7.3 - 91	36 - 100
Bottom Time (min)	5.0 - 350	19 - 287
Dive Time (min)	9.5 - 300	19 - 287

The distribution of the bubble grade data are: BG = 0 (no bubbles detected) > 40%; BG = 1 and 2 (low bubble activity) < 30%; and BG = 3 and 4 (high bubble activity) < 30%. The advantage of these data is that they are fairly evenly distributed in contrast to the typically low occurrence of DCS. We purposely grouped bubble grades (i.e., 1 & 2, and 3 & 4) from the original 5 categories for modeling purposes, as explained below.

Model

We assume that the maximum predicted bubble size correlates with the maximum recorded bubble grade. The model does not take into account the times of occurrences of these maxima. The method of maximum likelihood estimation is used to fit the parameters using a modified Marquardt algorithm (Bailey and Homer 1977).

The bubble model is documented elsewhere (Tikuisis et al. 1994, Gault et al. 1995); hence, only key points will be presented here. The gas flux depends on the concentration difference between the gas in the bubble and that outside the

bubble in the tissue or fluid, and on the rate constant representing a diffusion barrier to gas transfer across the gas-bubble interface:

$$J_i = k_i \cdot \Delta C_i \tag{1}$$

where J is the gas flux, k is the rate constant, and ΔC is the gas concentration difference across the bubble interface for gas 'i'. The gas content of the bubble, N^g, is constrained by a mass balance and the amount of gas leaving or entering the bubble depends on the gas flux:

$$\frac{dN_i^g}{dt} = 4\pi R^2 \cdot J_i \tag{2}$$

Finally, tissue gas exchange with the blood is assumed to be perfusion-limited and is characterized by a time constant, τ, according to (Hills 1977):

$$\frac{dP_i}{dt} = \frac{P_i^{bl} - P_i}{\tau_i} \tag{3}$$

where P is the gas tension and the superscript 'bl' refers to its value in blood.

We now present the probability functions used to predict bubble grades. First, we consider the simpler binomial case. If our purpose was only to predict incidences of low versus high BG, the following expressions would suffice:

$$Pr_{lowBG} = e^{-a \cdot R_{max}}$$
$$Pr_{highBG} = 1 - e^{-a \cdot R_{max}} \tag{4}$$

where Pr is the probability of a BG outcome, as illustrated in Fig. 1. The prediction of low BG prediction is a single parameter estimation involving R_{max} as an exponent. Clearly, predictions of a high incidence of low BG are associated with low values of R_{max}. Conversely, a high incidence of high BG is associated with large values of R_{max}. By definition, the two probabilities sum to unity. This binomial approach to BG prediction is analogous to the prediction of DCS.

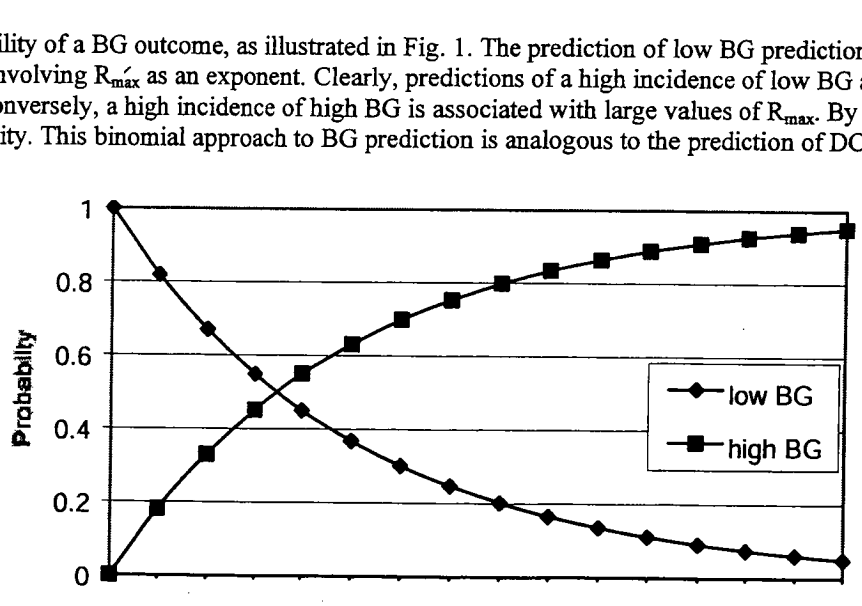

Figure 1. Illustration of the binomial probability function.

To provide a more elaborate prediction, an additional probability function was introduced to allow a trinomial outcome (based on advice from Dr. L.D. Homer). This allowed a separate prediction of BG = 0, as follows:

$$\begin{aligned} Pr_{BG=0} &= e^{\frac{-a \cdot R_{max}}{b}} \\ Pr_{BG=\{1,2\}} &= e^{\frac{-R_{max}}{b}} - e^{\frac{-a \cdot R_{max}}{b}} \\ Pr_{BG=\{3,4\}} &= 1 - e^{\frac{-R_{max}}{b}} \end{aligned} \qquad (5)$$

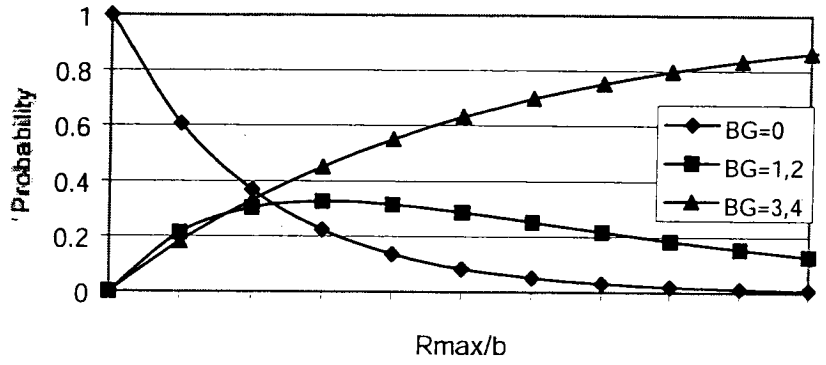

Figure 2. Illustration of the trinomial probability function (Eq. 5).

Close examination of the low BG (= 1, 2) prediction reveals that a second parameter, b, has been introduced, and the shape of this probability function is distinctly different from the other two. Yet, the summation of all probabilities to unity is preserved.

Figures 3 and 4 demonstrate the influence of parameter 'a' on the probability distributions. Low values of 'a' suppress the prediction of low BG. A higher value will boost the maximum probability of low BG allowing the possibility that the probabilities of the other two outcomes can be exceeded within a certain range of R_{max}.

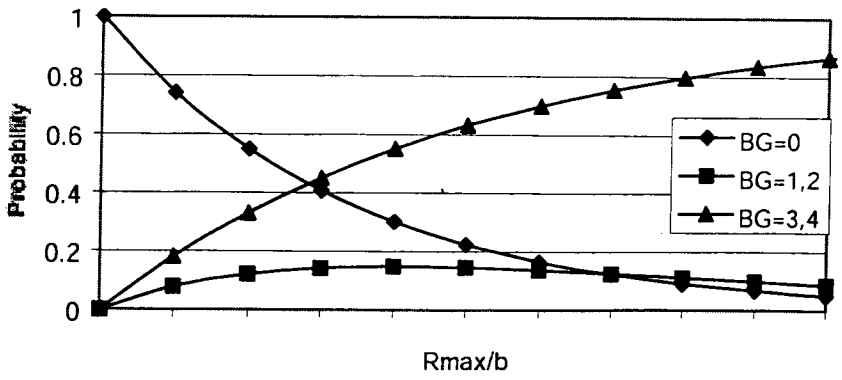

Figure 3. Illustration of the trinomial probability function with a low value of 'a'.

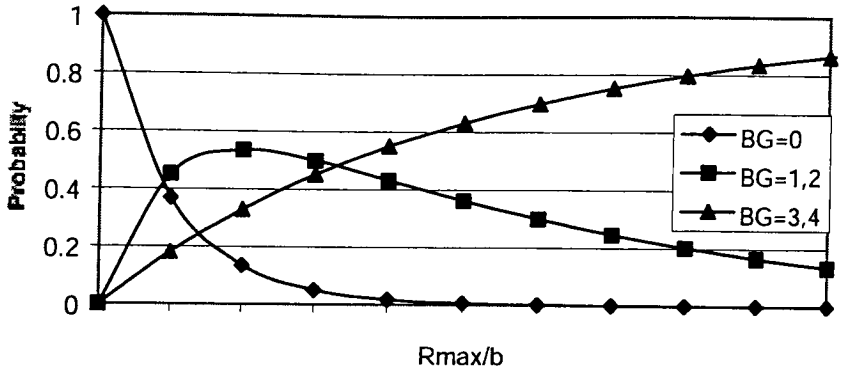

Figure 4. Illustration of the trinomial probability function with a high value of 'a'.

The likelihood function, L, is the product of the above probabilities, each raised to the power of the number of times, N, that the corresponding Doppler score was observed, i.e.:

$$L = Pr_{BG=0}^{N_0} \cdot Pr_{BG=\{1,2\}}^{N_{1,2}} \cdot Pr_{BG=\{3,4\}}^{N_{3,4}} \qquad (6)$$

For computational convenience, the logarithm of L is used for parameter estimation:

$$LL = \sum N_0 \cdot \ln Pr_{BG=0} + N_{1,2} \cdot \ln Pr_{BG=\{1,2\}} + N_{3,4} \cdot \ln Pr_{BG=\{3,4\}} \qquad (7)$$

Since all probabilities are less than or equal to zero, maximum likelihood is attained when LL has the lowest possible negative value.

The complete list of model parameters are the time constant of the tissue (τ), the rate constant of gas transferring in and out of the bubble (k), the gas solubility in tissue (δ), the volume of the tissue surrounding the bubble (v), the surface tension of the bubble (γ), and the two scaling parameters (a, b). The expression that relates the gas solubilities and tissue volume is given in Tikuisis et al. (1994) and Gault et al. (1995), and primarily involves the minimum bubble size condition for bubble growth. The rationale for the other parameter choices are also presented in the cited references.

Results

Table 2 summarizes the variety of model configurations used to achieve the best fit of the data.

Table 2. Summary of model parameters used (√) and corresponding maximum log Likelihood values. Two estimates (for nitrogen and helium) were made for k and δ, where indicated by a √.

Parameters							LL
τ	k	δ	ν	γ	a	b	
							-2,229.7*
√	√					√	-2,189.1
√	√				√	√	-2,181.8
√	√	√				√	-2,158.9
√	√	√			√	√	-2,149.4
√	√	√	√	√	√	√	-2,146.4

**null model estimation*

The nine-parameter version (see Table 3) yielded the most significant improvement according to the log-likelihood ratio test. Note that the time constants of nitrogen and helium are markedly different, but their relative order is consistent with expectation. However, the large difference in gas solubilitities between the two gases suggest different tissue types. This is problematic but not surprising considering that the fit was performed on a single tissue (lack of data precluded the use of additional model tissues). The estimated value for the tissue volume is within the range used by other researchers. The very low estimated surface tension concurs with values reported by Paul Weathersby et al. (1982).

Table 3. Summary of model parameter estimates (± SE) of the best fit. The estimate of τ for helium was derived from the value for nitrogen.

Parameters	Nitrogen	Helium
τ (min)	27.9 ± 1.9	9.3 ± 8.3
k ($cm \cdot s^{-1}\ 10^{-6}$)	0.050 ± 0.013	55.5 ± 120
δ	0.0438 ± 0.0002	0.0096 ± 0.0079
ν ($cm^{-1}\ 10^{-4}$)	3.6 ± 0.9	
γ (dyne cm^{-1})	5.0 ± 2.2	
a	2.55 ± 0.09	
b ($cm\ 10^{-2}$)	1.39 ± 0.16	

Discussion

How well does the model fit bubble observations outside the calibration data set? We begin our examination of this question with a 45-meter seawater (msw) dive on air for 30 min. This was an experimental dive which involved sedentary divers half immersed in cold water, very unlike the dives in the data set used for the model calibration. As can be seen in Fig. 5, the model prediction is poor. This illustrates the model's lack of generality and risk of overextrapolation.

The next dive examined was similar, but involved working dives conducted on a semi-closed circuit breathing apparatus. Better agreement was obtained in this case. The next dive examined was a 45 msw for 30 min on heliox, and a similar level of agreement between the observed and predicted BG was attained as with the previous air dive. The last dive examined was a 15 msw for 4 days saturation dive where no bubbles were detected, in accordance with the model prediction of a zero bubble grade.

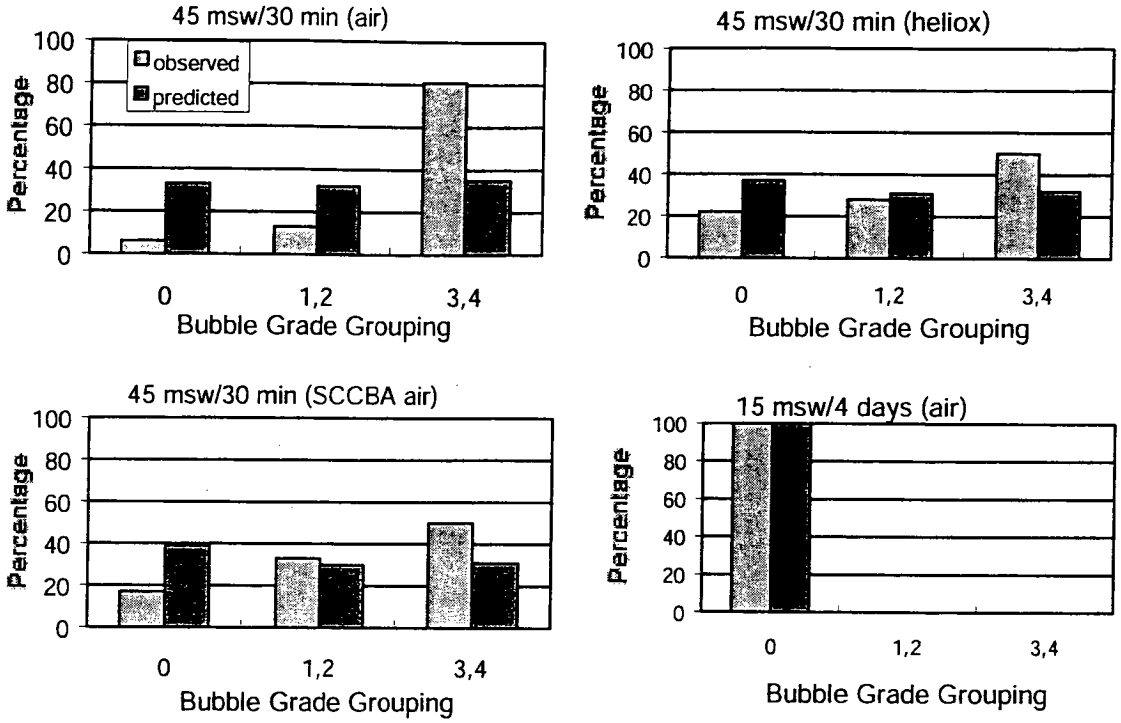

Figure 5. Comparison of observed and predicted bubble grades for various dives.

Although we have not used any time of occurrence information in the model estimation, it is informative to compare the evolution of predicted bubble sizes and observed bubble grades. The dive profile examined for this purpose in Fig. 6 is a 45 msw for 50 min dive on air. Superimposed on the plot of bubble radius are bubble grades for the six divers (identified by numbers 1 through 6) involved in this trial. For example, diver #1 had BGs of 0, 3, and 4 at about 70, 120, and between 150 and 220 min, respectively, and then BG began to decrease. Indeed, the history of all the divers' BGs tend to be described by the shape of the predicted bubble radius envelope. This reasonably strong chronological correlation is remarkable considering that the parameter estimations were based on the maximum bubble grade recorded, not on when it occurred or on the events preceding or following the maximum occurrence.

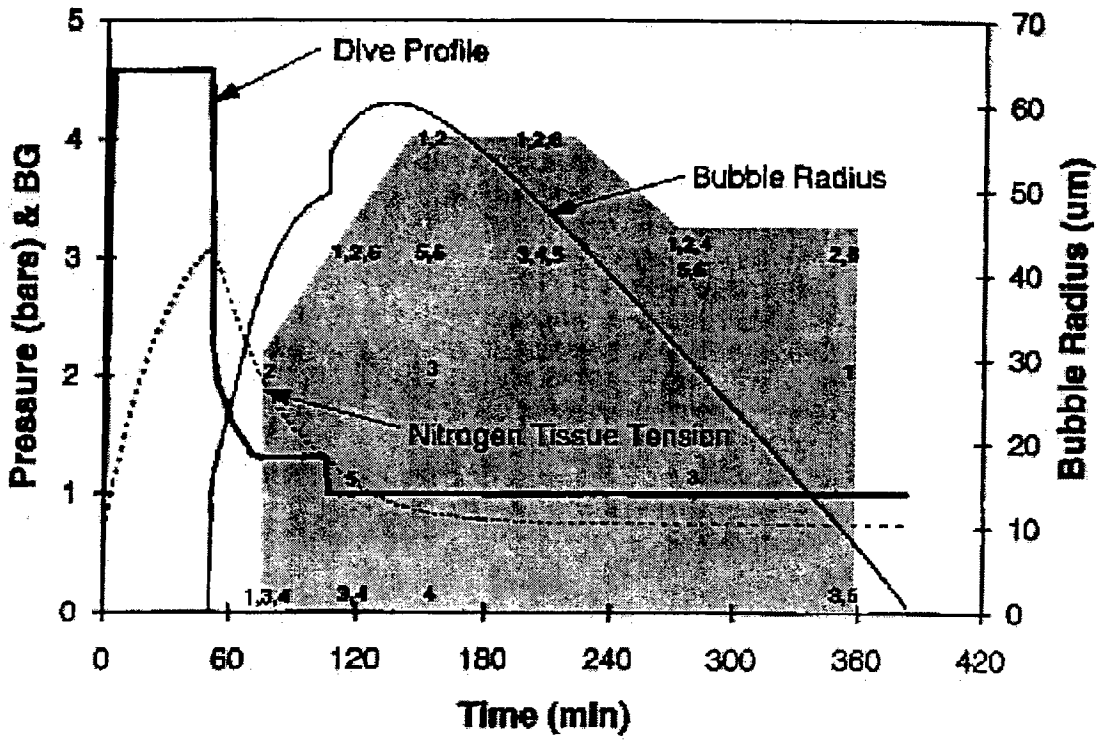

Figure 5. Comparison of observed and predicted bubble grades for a 45 msw for 50 min dive on air. The heavy solid line defines the dive profile; the dotted line shows the predicted tissue gas tension; the thin solid line shows the predicted bubble radius; and the numbers within the shaded region refer to the diver's identification and indicate the BGs recorded (scale on left axis).

Summary

The present model distinguishes three levels of intravascular bubble activity and represents a departure from the binomial outcome distribution usually applied in the prediction of DCS. It can be referred to as a 'competing risk' model according to the co-chair's (Dr. W.A. Gerth) overview.

Although we have some difficulties with the interpretation of some of the model parameter estimates, they fell within the range of acceptable human biological values. The strong chronological correlation between the maximum predicted bubble size and the maximum recorded bubble grade is important. This is because the time of these maxima lagged the occurrence of maximum gas super-saturation which generally occurs upon surfacing and has been considered representative of the maximum instantaneous risk of DCS. The bubble model prediction is consistent with the general observation that DCS symptoms usually occur after surfacing.

References

Bailey, R.C. and Homer, L.D. (1977). An analogy permitting maximum likelihood estimation by a simple modification of general least squares algorithms. Naval Medical Research Institute Report No. 86-51, Bethesda, MD.

Nishi, R.Y. (1993). Doppler and ultrasound bubble detection. In: Bennett, P.B. and Elliott, D.H. (eds.) The Physiology and Medicine of Diving. Saunders, London, pp. 433-453.

Tikuisis, P., Gault, K.A. and Nishi, R.Y. (1994). Prediction of decompression illness using bubble models. Undersea Hyperbaric Med. 21:129-143.

Gault, K.A., Tikuisis, P. and Nishi, R.Y. (1995). Calibration of a bubble evolution model to observed bubble incidence in divers. Undersea Hyperbaric Med. 23:249-262.

Hills, B.A. (1977). Decompression sickness, Vol 1: The biophysical basis of prevention and treatment. John Wiley & Sons, New York.

Weathersby, P.K., Homer, L.D. and Flynn, E.T. (1982). Homogeous nucleation of gas bubbles in vivo. J. Appl. Physiol. 53:940-946.